ELSEVIER

External cavity multiwavelength superbroadband diode laser

I.S. Moskalev[a,*], S.B. Mirov[a], V.V. Fedorov[a], T.T. Basiev[b]

[a] *Department of Physics, Laser and Photonics Research Center, University of Alabama at Birmingham, 1300 University Blvd.,*
Birmingham, AL 35294, USA
[b] *General Physics Institute, Russian Academy of Sciences, 38 Vavilov St., Moscow 117942, Russia*

Abstract

Multiwavelength semiconductor laser source for dense wavelength division multiplexing (DWDM) applications based on a novel dispersive cavity is described. Multiline lasing on the basis of a single-diode laser chip and multi-stripe diode laser is analyzed theoretically and demonstrated experimentally. Simultaneous lasing across ∼80% of the FWHM of the luminescence bandwidth of the AlGaAs active medium (657–667 nm) in multiline regime with a special pre-assigned spectral composition was realized. For DWDM applications a prototype of this superbroadband semiconductor laser operating in one of the telecommunication wavelength bands around 1.5 μm has been designed on the basis of a multi-stripe diode chip. Simultaneous lasing of four spectral lines in the region 1567–1577 nm has been obtained.
© 2003 Elsevier Science B.V. All rights reserved.

1. Introduction

Dense wavelength division multiplexing (DWDM) promises to greatly expand the capacity of optical fibers, both those yet to be installed, and perhaps more importantly, those already deployed in terrestrial and undersea systems. For viable DWDM systems, low cost laser sources maintaining accurate adherence to the particular channel wavelength spacing are required. As the

channel spacing of DWDM network decreases, short-cavity lasers, such as distributed feedback (DFB) lasers, distributed Bragg reflector (DBR) lasers, and vertical cavity surface emitting lasers (VCSELs), may have to be externally wavelength stabilized to control the temperature dependent output wavelength drift. To improve the wavelength stability one can use a longer external cavity and produce a diffractively stabilized lasing wavelength separation. Examples of these lasers include multichannel grating cavity lasers with bulk-optic [1–4] and integrated design [5–7]. However, some of those systems lack flexibility in the selection of wavelengths, total amount of available channels, and wavelength spacing. In addition to that, a

---

* Corresponding author. Tel: +1-205-934-5318; fax: +1-205-934-8042.

E-mail address: moskalev@phy.uab.edu (I.S. Moskalev).

compensation for optical crosstalk can be a significant issue.

This paper describes theoretical analysis and practical realization of a new type of source – a multiline superbroadband (ML/SB) diode laser for use in DWDM systems. It is based on a novel external cavity construction where optical components of the cavity maintain distinct gain channels in a single- or a multi-stripe diode chip, reduce crosstalk, suppress mode competition, and force each channel to lase at a specific stabilized wavelength. By designing this cavity structure appropriately, the system creates its own microcavities each lasing at a different wavelength across the complete gain spectrum of the active material. Recently we demonstrated a true superbroadband and multiline lasing of a color center laser [8–13] with a spectral width practically coinciding with the luminescence spectrum of the gain medium. Now we demonstrate an application of this novel cavity design to build a ML/SB laser based on a conventional Fabry–Perot diode chip. The construction of the cavity is flexible and also allows utilization of multi-stripe diode chips, diode arrays, as well as individual diode lasers. The laser could be readily integrated with external modulators. With a multi-stripe diode chip or a diode array cavity a current modulation of individual channels can be realized, being limited only by the cavity roundtrip and carrier recombination times.

2. Background. Multiline superbroadband laser. Principles of operation

The basic optical scheme of the laser cavity is shown in Fig. 1. It consists of input coupler M_1, active element, spatial mask, intracavity lens L_1, aperture A installed in the lens focal plane, and a diffraction grating G operating in the Littrow mount scheme. The laser works in the following way.

Emission from the active medium passes through the spatial mask where it is split into a number of beams – channels. The beams are refracted on the focusing lens L_1 and focused onto the off-axis mode suppression element – aperture A. The aperture separates and transmits only the
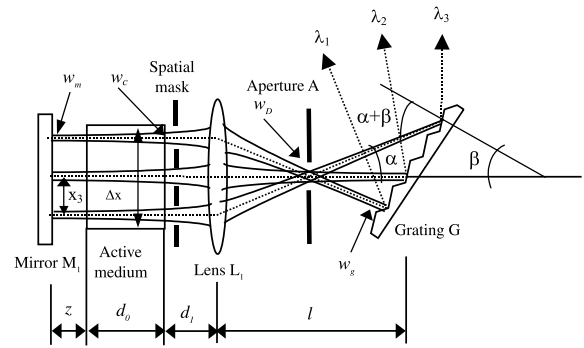

Fig. 1. General design of the multiline superbroadband laser (see description in Section 2).

part of the radiation that propagates parallel to the resonator optical axis on the left shoulder of the cavity. The transmitted radiation is diffracted on the diffraction grating G and, therefore, every wavelength goes along its own unique direction. The grating, that has only the zeroth and the first orders of diffraction, is positioned in the Littrow mount configuration. The zeroth order serves for the laser output. The first order of the diffracted light is retroreflected to the aperture, which extracts from it only the main laser modes. The high order modes, which diverge from corresponding optical axes of the channels, are expelled from the process of generation. Hence, the aperture must simultaneously select the fundamental transverse modes for all existing channels in the cavity. It is done by positioning the aperture in the place where all the channels intersect – the focal plane of the lens L_1. The width of the aperture is estimated as the mode size in that plane.

The radiation of the main laser modes, each with a distinct wavelength, is collimated by the focusing lens and directed back to the active medium. Each mode with its specific wavelength has its own trajectory confined within a channel defined by the corresponding opening in the spatial mask and the intracavity aperture. This radiation, along with the stimulated radiation provoked by it, is reflected directly back by the mirror M_1. This process gives rise to the superbroadband multiline lasing, where different wavelengths are amplified in different regions of the active element. The overall

output bandwidth is determined by parameters of the cavity optical elements and may coincide with active medium amplification band.

The spatial mask selects the active cavities (active wavelengths). Choosing parameters of the mask (size of its holes and their separation) one can set a certain spectral structure of the output radiation. Furthermore, one can tune the laser wavelengths by simply moving the mask in transverse direction. The spatial mask, in conjunction with other optical components of the cavity, has the same functional role as multiple stripes in diode structures. However, it provides an additional flexibility in choosing output spectral composition from the amplification band of the gain medium. When the mask is removed the output spectrum consists of a grid of narrow spectral lines. In that case, if the linewidths of individual lines are larger than the spectral separation between the lines, one observes a continuous, superbroadband output spectrum as demonstrated for color center lasers in [9–13].

If we assume that, according to Fig. 1, each beam passing through active element is located at a coordinate x in the transversal direction with respect to the position of the optical axis of the laser, the angle of intersection of the current beam x and the optical axis α is small (paraxial approximation), and the focal length of the focusing lens L_1 is f, then we can write

$$\alpha \approx \frac{x}{f}. \tag{1}$$

If the normal to the diffraction grating forms an angle β to the optical axis then each beam x arrives at the diffraction grating at an angle $\beta + \alpha$.

Each beam striking the diffraction grating at a specific angle has a specific wavelength determined from the well-known Littrow mount condition

$$k\lambda = 2t \sin(\beta + \alpha), \tag{2}$$

where k is the order of diffraction ($k = 1$ in this case), and t is the grating spacing period. The angle β is defined from the autocollimating condition for the central wavelength λ_0

$$\beta = \arcsin\left(\frac{\lambda_0}{2t}\right). \tag{3}$$

Using (1)–(3) one finds that each active zone of the crystal located at a distance x_i from the optical axis (Fig. 1) generates its own wavelength λ_i determined as

$$\lambda_i \approx 2t \sin\left(\arcsin\left[\frac{\lambda_0}{2t}\right] + \frac{x_i}{f}\right). \tag{4}$$

For a stable cavity depicted in Fig. 1, adjacent laser modes do not overlap with each other inside the gain medium. This results in an independent oscillation of the different parts of active medium at different wavelengths covering a spectral region of the gain medium amplification band determined by the parameters of the cavity optical elements and their mutual disposition in the cavity.

Eq. (4) shows that wavelength of a particular channel λ_i is a function of its coordinate x_i in the crystal. Considering λ as a continuous function of x and taking the derivative $d\lambda/dx$ at $x = 0$ (optical axis) we obtain the overall spectral bandwidth of the output radiation

$$\Delta\lambda \approx \frac{2t\Delta x}{f} \cos\left(\arcsin\left[\frac{\lambda_0}{2t}\right]\right), \tag{5}$$

where Δx is the transverse size of the crystal. The diffraction grating period t should be chosen as small as possible to achieve the highest spectral resolution of the cavity. Therefore, it can be assumed that the output bandwidth is the function of the crystal size and focal length of the lens only. Using the appropriate lens for a given laser crystal it is possible to cover either the whole amplification band of the laser material or any portion of it.

In this paper we describe two multiline diode lasers based on AlGaAs diode chips operating in the region of 657–667 and 1560–1580 nm. The dimensions of their p–n junctions are $500 \times 100 \times 1$ μm and $2000 \times 2000 \times 1$ μm, correspondingly. The diffraction gratings used in the experiments were 1800 and 1200 grooves/mm for the visible and the infrared lasers, respectively. The overall output bandwidths $\Delta\lambda$ versus the focal length f of the intracavity lens for the crystals and gratings used in the experiments are shown in Fig. 2. These dependencies can be used for choosing the required focal length of the intracavity lens for a given output spectrum bandwidth, as we do in our experiments. In the following section we develop a
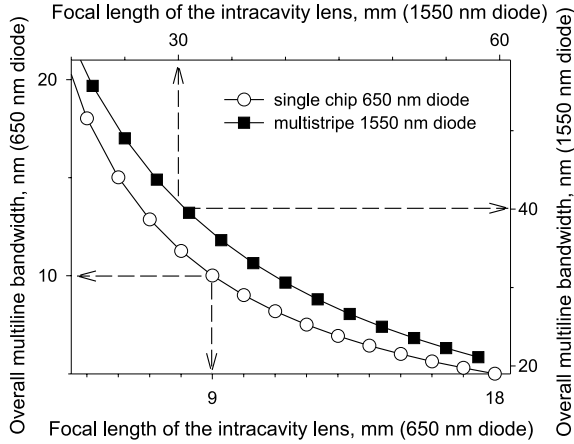
Fig. 2. Overall output bandwidth as a function of focal length of the intracavity lens for the visible and infrared diodes. The circle-symbol curve plotted against the left y axis and bottom x axis corresponds to the visible laser; the filled square-symbol curve plotted against the right y axis and the top x axis corresponds to the infrared laser.

simple model of the ML/SB laser and establish the relations between the parameters of the optical elements as well as their locations in the cavity.

3. Simple model of the superbroadband diode laser in multiline output mode

In the simplest model of the ML/SB laser the laser cavity consists of two plane mirrors, intracavity lens and a dielectric slab that represents the active element. In this model the diffraction grating, operating in the autocollimation regime, is equivalent to a plane mirror. This model is applied for each channels of the laser.

The cavity analysis is based on the matrix method for Gaussian beams [14,15]. The matrix of an equivalent resonator is calculated as follows:

$$M = \begin{pmatrix} 1 & l \\ 0 & 1 \end{pmatrix} \begin{pmatrix} 1 & 0 \\ -1/f & 1 \end{pmatrix} \begin{pmatrix} 1 & d_{\text{eff}} \\ 0 & 1 \end{pmatrix}$$
$$= \begin{pmatrix} g_1 & L \\ (g_1 g_2 - 1)/L & g_2 \end{pmatrix}, \tag{6}$$

where $d_{\text{eff}} = z + d_0/n + d_1$ is the effective distance between mirror M_1 and the lens L_1, and z is the separation between the mirror and the rear facet of

the crystal, d_0 is the length of the crystal, d_1 is the distance from the output facet of the crystal to the lens, and n is the refraction index of the active medium.

The resonator effective length L is given by

$$L = d_{\text{eff}} + l - \frac{l d_{\text{eff}}}{f}, \tag{7}$$

where l is the separation between lens L_1 and grating G, and f is the focal length of the lens. The parameters $g_1 = 1 - l/f$ and $g_2 = 1 - d_{\text{eff}}/f$ are the stability parameters of the resonator.

An unstable cavity configuration leads to a strong overlapping and coupling among different channels. Therefore, we consider only stable cavity configurations for which the following stability condition is satisfied:

$$0 < g_1 g_2 < 1. \tag{8}$$

The beam radii of TEM_{00} modes for individual channels at the mirror w_m, the diffraction grating w_G, output crystal facet w_c, and the aperture w_D are calculated via the ABCD law for the appropriate cavity unit cells [14,15]

$$w_m^2 = \left(\frac{L\lambda}{\pi}\right)\sqrt{\frac{g_2}{g_1(1 - g_1 g_2)}}, \quad w_G^2 = w_m^2 \frac{g_1}{g_2}, \tag{9}$$

$$w_c^2 = w_m^2 + \frac{\lambda^2(z + d_0/n)^2}{\pi w_m^2}, \quad w_D = \frac{\lambda f}{\pi w_m}, \tag{10}$$

where a beam radius is defined as the radius where intensity of the mode is decreased to $1/e^2$ of its maximum.

In order to avoid crosstalk the channels should not overlap in the active medium. The minimum channel's overlapping and maximum amount of oscillation lines can be realized by minimizing beam radius on the output facet of the laser crystal w_c. It follows from (10) that the minimum beam radius is achieved with $z = 0$ and

$$w_c^2 = 2w_m^2 = \frac{2\lambda d_0}{n\pi}. \tag{11}$$

The maximum number of oscillation channels can be estimated as the ratio of the crystal width to the beam diameter on the output facet of the crystal $N = \Delta x / 2w_c$. The spectral separation of the channels is found using (5), where Δx is replaced

by the spatial separation of the channels, which, in turn, equals the channels diameters on the output facet of the crystal

$$\delta\lambda = \frac{4tw_c}{f}\cos(\beta),\qquad(12)$$

where β is the autocollimation angle for the central wavelength of the amplification band (see (3) and Fig. 1).

In order to avoid channel's crosstalk the diffraction grating must provide spectral resolution better than or equal to that given by (12). The diffraction grating resolution is determined by the number of illuminated grooves and can be calculated in terms of the beam diameter on the grating

$$\delta\lambda_G = \frac{\lambda t}{2w_G}\cos(\beta).\qquad(13)$$

The requirement on the diffraction grating resolution $\delta\lambda_G \leqslant \delta\lambda$ leads to the following condition on the minimum mode diameter on the diffraction grating:

$$w_G \geqslant \frac{\lambda f}{8w_c}.\qquad(14)$$

The requirements on the laser cavity parameters discussed above can be conveniently summarized in three expressions in terms of the cavity stability parameters g_1 and g_2 as follows.

The requirement of the cavity stability (8)

$$g_1 > \frac{1}{g_2}.\qquad(15)$$

The requirement of the minimum resolution of the diffraction grating (14)

$$g_1 \leqslant \frac{\pi}{128A^2}.\qquad(16)$$

The requirement of the maximum number of channels (9) and (11)

$$g_1 = \frac{g_2}{g_2^2 + A^2},\qquad(17)$$

where $A = d_0/(nf)$. All possible cavity configurations are determined by these three expressions and for a given laser crystal the only independent variable is the focal length of the intracavity lens.

Fig. 3 shows a typical stability diagram for the diodes used in the experiments. All possible
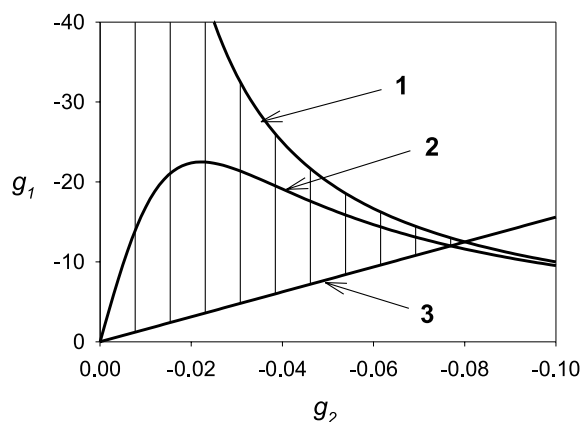

Fig. 3. Stability diagram of the diode lasers. All stable cavities with the appropriate cavity spectral resolution are located within the shaded area between curve 1 (Eq. (15)) and straight line 3 (Eq. (16)). The cavities that provide maximum number of channels are represented by the curve 2 (Eq. (17)).

cavity configurations are confined by the stability boundary (15), the straight line (16), that represents the requirement of the minimum grating resolution, and those configurations that provide maximum number of channels fall onto the curve (17). Once the diagram is created, one can find the desired cavity length and position of the lens (whose focus was found from (5) and Fig. 2).

In our experiments the goal was to utilize the whole luminescence bandwidths of the diodes (10 nm for the visible laser and 40 nm for the infrared, correspondingly) and obtain the maximum number of output channels. The required focal lengths of the intracavity lenses are 9 and 30 nm for the visible and the infrared lasers, respectively (see Fig. 2). From the stability diagrams we find the appropriate cavity configurations of the lasers. The optimal channel diameters $2w_c$ for the crystals are 16 and 50 μm for the visible and the infrared lasers, respectively. This results in the maximum quantities of independent channels for these diodes of $N \sim 6$ and $N \sim 40$ for the visible and the IR lasers, respectively. In the following section we present the experimental results for the two semiconductor multiline lasers and analyze the extent of their agreement with the theoretical predictions obtained above.

4. Experimental results

The schematic diagram of the experimental set-up is shown in Fig. 4. Instead of a single intracavity lens a double-lens focusing system was used. The focusing system consists of a spherical microobjective L_1 and a cylindrical tuning lens L_2. For diode lasers such an arrangement was found to be more convenient for the following reasons. The microobjective is used to collimate the highly divergent output radiation of the diode in the vertical plane (fast axis of the diodes). In the horizontal plane (slow axis of the diodes) the focusing system works as an equivalent single intracavity lens with variable focal length that significantly simplifies the adjustment procedure. For transverse-mode selection we used a variable slit located at the point of intersection of the beams, which is located near the focal point of lens L_1.

The theoretical analysis given in previous sections is extended to this particular experimental setup as follows. In the matrix analysis the single thin lens matrix is replaced with a matrix of a two-lens telescope whose required effective focal length is determined in exactly the same way as shown in the previous section. The effective focal length of the telescope f_{eff} consisting of two lenses f_1 and f_2 separated by a distance l_T is defined as

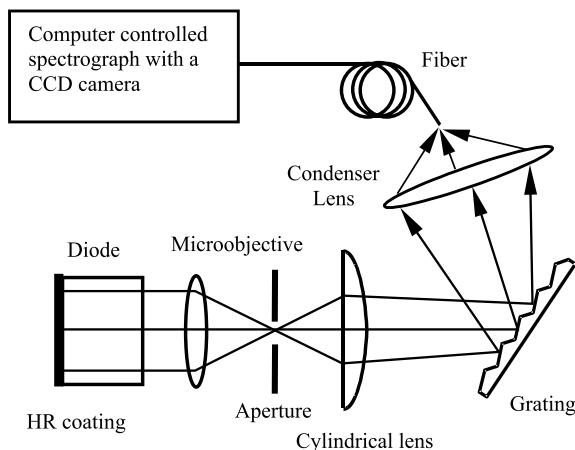$$\frac{1}{f_{eff}} = -\frac{1}{f_1} - \frac{1}{f_2} + \frac{l_T}{f_1 f_2}. \tag{18}$$

Fig. 4. Schematic diagram of the experimental setup (see description in Section 4).

The positions of the telescope lenses are calculated based on the requirements for the effective focal length of the intracavity telescope and the conditions (15)–(17) for the laser stability, spectral resolution, and maximum number of output channels.

For the measurements of the output spectrum of the visible laser the "Acton Research Corporation SpectraPro-150" spectrograph with "Princeton Instruments TEA/CCD-1024 EM/1" CCD camera was used. For the spectrum control of the IR laser output we used "Acton Research Corporation SpectraPro-300i" spectrometer with a PbS detector. The approximate resolution of the spectrometers is 0.5 nm. For a high resolution measurements we used two Fabry–Perot etalons with finesse of 14 and a free spectral ranges of 47 and 1 cm^{-1}, respectively.

The multiline outputs along with the luminescence spectra for both diodes are shown in Fig. 5. The output spectrum of the visible laser is depicted in Fig. 5(a). The luminescence spectrum of the visible laser is centered at 660 nm and has a bandwidth of about 20 nm at the $1/e^2$ level. The overall bandwidth of the simultaneous oscillation of five spectral lines is about 8 nm, which constitutes ~80% of the FWHM of the luminescence bandwidth of the active medium. The average line separation is approximately 1.6 nm. Comparison of these results with our theoretical predictions in the previous section shows that our laser model, although very simplified, is in a good agreement with the experiments.

The results for the multi-stripe infrared laser are shown in Fig. 5(b). The luminescence bandwidth is about 40 nm and the overall multiline bandwidth is approximately 8 nm with spectral separation of about 2 nm. The disagreement of the experimental results and our theoretical predictions for this laser is due to the following reasons. First of all, the front facet of the laser chip has a reflection of 4% which, along with 100% back facet, causes a strong coupling between the external cavity and the cavity formed by the laser chip facets. In this situation, each stripe of the laser together with the external cavity forms an external cavity diode laser with a weak feedback. In this case we expected to obtain at most five oscillation lines separated by 10 nm (as shown in the previous section). We were able to use only four stripes out of five. The reason for
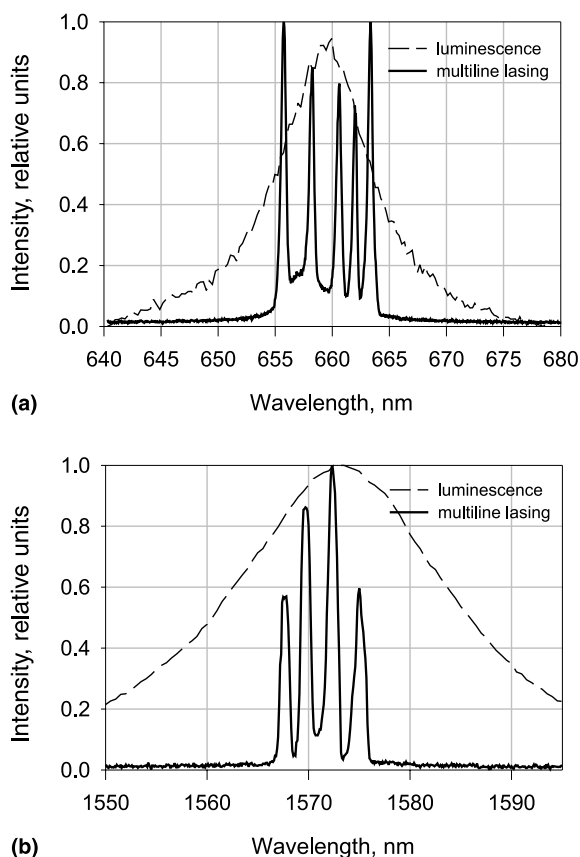
(a)

(b)

Fig. 5. Multiline operation of ML/SB diode laser along with the luminescence spectrum: (a) visible 650 nm single-chip diode laser; (b) infrared 1550 nm multi-stripe diode laser.
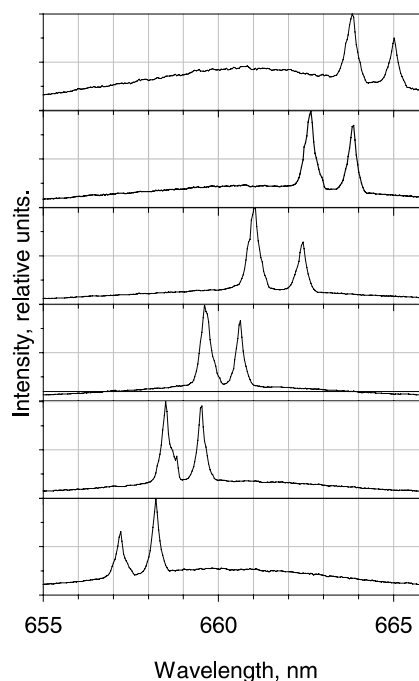

Fig. 6. Tunable dual-wavelength operation of the visible ML/SB diode laser. The tuning range of the dual-wavelength operation corresponds to the FWHM of the laser amplification band. The tuning is performed by manual rotation of the diffraction grating in the plane of its dispersion.

that is that the total transverse size of the multistripe laser chip (2 mm) is of the order of the microobjective clear aperture (4.5 mm). This causes a significant spherical aberration resulting in a huge intracavity loss for one of the side stripes. Still, this experiment shows that it is possible (and even preferable) to use a multi-stripe diode chip as a basis for the ML/SB laser.

Fig. 6 shows a tunable dual-wavelength visible diode laser operation. This operation regime has been obtained by the adjustment of the focusing system to create only two oscillation channels in the active medium (by changing separation between lenses L_1 and L_2). Rotation of the diffraction grating in the dispersion plane provides the tuning of the dual-wavelength laser oscillation. A dual-wavelength laser operation with 7 nm tuning range and with a constant 1 nm spectral distance between lines was achieved.

The spectral separation between oscillation lines can also be changed by tuning the effective focal length of the focusing system (as shown by (12)). The minimum spectral separation between lines in our experiments was approximately 0.008 nm (6.2 GHz). As one can see from Fig. 7, the linewidths of the oscillation lines, measured with a Fabry–Perot etalon, are less than 2.1 GHz, which is close to the free spectral range of the cavity (2.0 GHz). The spectrum in Fig. 7 also shows that at least one of the output spectral lines operates in a non-single longitudinal-mode regime. It is well-known that such a regime of operation of external cavity semiconductor lasers causes instability and linewidth broadening of the output radiation [16–20]. Those effects are mostly generated by intracavity parasitic reflections. Especially important are residual reflections from the output facet of the diode laser chip: the facet works as an additional
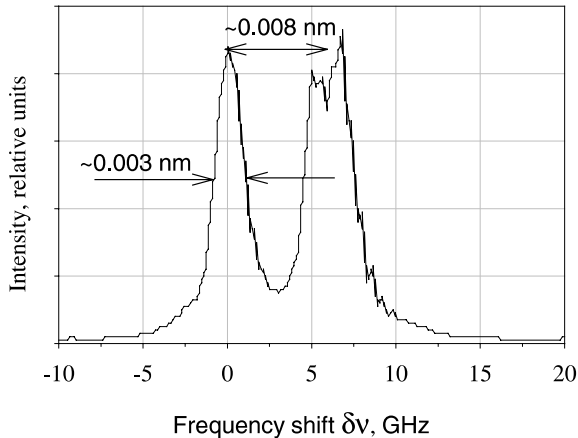
Fig. 7. High resolution measurement of a dual-wavelength output spectrum obtained with a Fabry–Perot interferometer. The spectrum demonstrates that one of the channels operates in the single longitudinal regime; the other spectral line consists of two longitudinal modes. The spectral lines are separated by approximately 0.008 nm (6 GHz) and the linewidth of the narrowest channel is less than 0.003 nm (2 GHz).

laser mirror, which causes formation of a complex multiple coupled cavities. Therefore, to obtain stable, single longitudinal-mode operation of every channel of the multiline laser it is crucial to use diode chips with high quality AR-coated output facets.

In this paper we demonstrate feasibility of re-alization of a novel DWDM laser source based on conventional, commercially available semiconductor laser chips and a new spatially dispersive cavity described above. Improvement of the laser performance, in particular, obtaining a narrow linewidth, single transversal- and longitudinal-mode operation of each spectral channel, reduction of channels crosstalk and increasing of the high order modes suppression ratio, is the subject of our future investigations.

5. Conclusions

In this paper we have analyzed theoretically and demonstrated experimentally a multiline super-broadband diode laser based on a novel laser resonator scheme. Multiline oscillation has been achieved with a single broad-stripe diode laser

operating at 660 nm and with a 1560 nm multi-stripe diode laser.

One of the major advantages of our laser scheme is that a large class of gain media can be used: a single-diode chip, a diode array or a multi-striped diode, solid state laser crystals, etc. With a properly prepared multi-stripe diode chip one can design a DWDM laser producing hundreds of spectral lines. For example, with a multi-stripe diode chip operating near 1550 nm, consisting of 100 stripes, 250 μm length and 10 μm width located at 5 μm from each other, one could build a 100-line ML/SB diode laser.

This paper demonstrates a promising and successful attempt to realize a multiline laser source for optical DWDM systems for telecommunication applications. The excellent reliability of the ML/SB laser combined with its remarkable ability to tailor a spectral response of arbitrary nature and the temperature stability of its grating stabilized external cavity make it a promising candidate for telecommunication applications.

Acknowledgements

References

[1] I.H. White, K.O. Nyairo, Electron. Lett. 26 (1990) 832.
[2] I.H. White, J. Lightwave Technol. 9 (1991) 893.
[3] G.C. Papen, G.M. Murphy, D.J. Brady, A.T. Howe, J.M. Dallesasse, R.Y. Dejule, D.J. Holmgren, Opt. Lett. 18 (1993) 1441.
[4] C.-L. Pan, C.-L. Wang, Opt. Quantum Electron. 28 (1996) 1239.
[5] J.B.D. Soole, K. Poguntke, A. Schere, H.P. LeBlanc, C. Chang-Hasnain, C. Caneau, R. Bhat, M.A. Koza, Electron. Lett. 28 (1992) 1805.
[6] M. Zirngibl, C.H. Joyner, L.W. Stulz, U. Koren, M.D. Chen, M.G. Young, B.I. Miller, IEEE Photon. Technol. Lett. 6 (1994) 516.
[7] C.R. Doerr, C.H. Joyner, L.W. Stulz, J.C. Centanni, IEEE Photon. Technol. Lett. 9 (1997) 1430.
[8] T.T. Basiev, S.B. Mirov, in: Laser Science and Technology Books Series, 16, Gordon and Breach Science Publishers/

Harwood Academic Publishers, London/New York, 1994, p. 1.

[9] T.T. Basiev, S.B. Mirov, P.G. Zverev, I.V. Kuznetsov, R.Sh. Tedeev, US Patent No. 5 (Oct. 1995) 461, 635.

[10] T.T. Basiev, P.G. Zverev, S.B. Mirov, Abstr. Rep. International Conf. LASER-93, Munich, Germany, 1993.

[11] T.T. Basiev, P.G. Zverev, S.B. Mirov, V.F. Fedorov, SPIE 2379 (1995) 54.

[12] T.T. Basiev, P.G. Zverev, V.F. Fedorov, S.B. Mirov, Appl. Opt. 36 (12) (1997) 2515.

[13] N.W. Jenkins, S.B. Mirov, OSA Trends in Optics and Photonics, vol. 34, Advanced Solid State Lasers OSA, Washington, DC, 2000, p. 364.

[14] N. Hodgson, H. Weber (Eds.), Optical Resonators Fundamentals, Advanced Concepts and Applications, Springer, London, 1977.

[15] A.M. Prokhorov (Ed.), Laser Handbook, Moscow, 1976.

[16] M.W. Fleming, A. Mooradian, IEEE J. Quantum Electron. QE-17 (1) (1981) 44.

[17] C.H. Henry, IEEE J. Quantum Electron. QE-18 (2) (1982) 259.

[18] P. Zorabedian, W.R. Trutna Jr., L.S. Cutler, IEEE J. Quantum Electron. QE-23 (11) (1987) 1855.

[19] J.-D. Park, D.-S. Seo, J.G. McInerney, Quantum Electron. 26 (8) (1990) 1353.

[20] C. Yan, X. Wang, J.G. McInerney, Quantum Electron. 32 (5) (1996) 813.